J Radiat Oncol (2013) 2:241–248
DOI 10.1007/s13566-012-0068-1

REVIEW

Utility of ^{18}FDG-PET/CT for head and neck cancer staging, radiation therapy planning, and follow-up

Amar U. Kishan · Partha Ghosh · Percy Lee

Received: 18 July 2012 / Accepted: 6 September 2012 / Published online: 15 September 2012

Abstract Radiation therapy (RT) is integral in the treatment of head and neck cancer (HNSCC), with intensity-modulated radiotherapy (IMRT) and other techniques allowing for more accurate and precise dose delivery to tumor while sparing normal tissues. ^{18}Fluorodeoxyglucose-PET, when used in concert with CT scanning (PET/CT), can assist in RT planning for HNSCC. First, PET/CT can identify additional foci of disease burden, changing radiation planning if not overall therapeutic intent. Second, PET data can influence gross tumor volume (GTV) delineation, typically producing smaller and more accurate target volumes. Consequently, dose escalation can be performed to a more limited tumor volume, either from the outset of therapy or at various times during an adaptive RT course. Follow-up PET/CT may be useful for early detection of recurrences and assessment of response after therapy; however, the optimal timing of the posttherapy study is still under investigation. A significant issue in the standardized use of PET/CT for RT planning remains the appropriate algorithm for segmenting the PET signal to delineate the GTV. Nonetheless, PET/CT-guided RT planning appears to pose multiple benefits for radiation oncologists and will likely continue to be an important advancement in the treatment of HNSCC with chemoradiotherapy.

A. U. Kishan
Harvard Medical School,
Boston, MA 02115, USA

P. Ghosh
Siemens Healthcare, Molecular Imaging,
Hoffman Estates, IL, USA

P. Lee (✉)
Department of Radiation Oncology,
David Geffen School of Medicine at UCLA,
200 UCLA Medical Plaza, B265,
Los Angeles, CA 90095, USA
e-mail: percylee@mednet.ucla.edu

Keywords PET/CT · Radiation therapy planning · Head and neck cancer

Introduction

Squamous cell head and neck cancer (HNSCC) is the sixth most common cancer worldwide, comprising 3 to 5 % of all cancers in the USA with over 50,000 new cases per year. Nearly 50 % of patients have advanced local disease or lymph node metastases at presentation. Therapeutic options include surgery, chemoradiation (CRT), and definitive radiotherapy (RT). Intensity-modulated radiotherapy (IMRT) utilizes steep dose gradients to conform the dose to target volumes, thereby limiting dose to organs at risk, and has become the RT technique of choice for HNSCC. Although CT-based RT planning is standard, CT only provides anatomical information. Since ^{18}fluorodeoxyglucose (FDG) positron emission tomography (PET) has an established role in diagnosis and staging in HNSCC, particularly when performed in a hybrid protocol with CT scanning (PET/CT), the incorporation of PET data into RT planning poses several advantages. First, by highlighting occult metastases or disease foci, PET data can change the goal of therapy. Similarly, it can also be used for disease surveillance and to monitor treatment response after chemoradiotherapy. Second, PET-derived metabolic tumor volumes (GTV_{PET}) may be more rational targets for therapy, as they likely represent functional tumor volumes. Third, as a corollary to this, dose escalation may be conducted to the GTV_{PET} only, allowing for delivering dose to metabolically most active area in order to increase tumor control. Here, we review the evidence for the benefit of PET/CT in the management of HNSCC, and additionally highlight different strategies use to segment RT target volumes based on PET data.

Identifying disease burden

Staging and therapeutic intent

Given its enhanced sensitivity and specificity for disease detection, PET/CT may influence initial treatment strategies by detecting occult disease (Fig. 1). In several studies, PET/CT led to TMN staging changes in 22–60 % of patients and RT planning changes in 29–57 % [1, 2]. A prospective study of 71 patients found that PET data led to management changes in 33.8 % of patients and detected additional sites of disease in 39.4 % [3]. Recently, the inclusion of PET data in a study of 24 patients identified two metastases and a second primary [4]. Notably, none of the five PET-positive/CT-negative nodes were malignant on pathology, underlying the measurable rate of false-positivity when staging is solely based on PET findings.

Recently, a multi-center study of 233 HNSCC patients prospectively compared therapeutic decisions based on conventional imaging (i.e., CT and MRI alone) or with additional PET data [5]. Staging was different in 43 % of patients and inclusion of PET data modified treatment in 13.7 %. The detection of metastatic disease was the primary method by which PET changed treatment intent. PET had less of an impact on treatment changes in this study compared to others, likely because fewer patients in this study had PET-detected occult metastases.

Despite the potential of PET to detect occult disease, its sensitivity may be relatively poor in some settings. In a meta-analysis including 1,236 patients with HNSCC, the sensitivity of PET alone without CT for nodal metastases in patients with a clinically N0 neck was only 50 %; i.e., there was pathologic lymph node involvement in half of the patients with negative PET scans [6]. Thus, PET imaging should not be considered an adequate imaging modality for monitoring clinically negative nodal regions. The limitation of PET in this setting could be related to the close proximity of the nodes to other FDG-avid structures, such as the major salivary glands, as well as the small size of occult nodal metastases.

Disease follow-up and treatment response

PET/CT data may also be useful for detecting residual disease or recurrence as well as response to radiotherapy (Fig. 2). Early studies employing PET scans alone found negative predictive values (NPVs) for residual nodal disease ranging widely from 50 to 100 %, while several recent studies have found consistently high (≥97 %) NPVs [7–9]. In a series of 65 patients followed for a median of 37 months, the NPV and specificity of PET/CT for residual nodal disease were 97 and 89 %, respectively [8]. In a subset of cases with no residual enlarged nodes by CT criterion, the NPV and specificity of PET increased to 98 and 96 %, respectively. These results suggest that a negative posttreatment PET/CT in patients without residual lymphadenopathy could mean that neck dissection can be safely withheld without compromising overall treatment outcomes; it can likely, but not definitely, be withheld for patients with a negative PET but with residual lymphadenopathy on CT alone. In 37 patients, spared neck dissection on the basis of a negative PET scan, none had developed recurrences by 18 months [7]. However, a recent study of 152 HNSCC patients with residual nodes >1 cm in axial dimension on CT following chemoradiotherapy found that PET/CT had only a 53 % sensitivity and 73 % NPV for having nodal disease

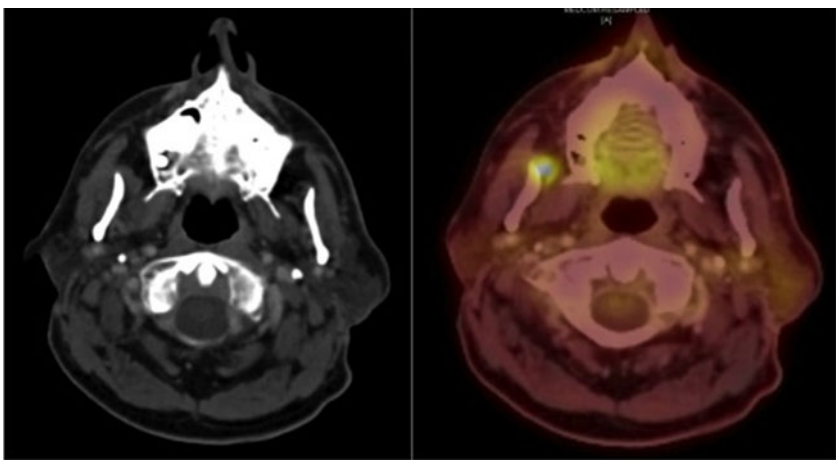

Fig. 1 A patient with a buccal mucosa squamous cell carcinoma with a pericentimeter ipsilateral occult nodal disease focus in a right submandibular lymph node. This involved lymph node and the primary tumor were treated with chemoradiotherapy. *Left*: contrast-enhanced CT scan in which the involved lymph node is not easily appreciated due its small size as well as adjacent dental artifacts. *Right*: co-registered FDG PET/CT demonstrated the intensely FDG-avid right submandibular lymph node helping to guide the radiotherapy targeting. Image courtesy of UCLA Department of Radiation Oncology, Los Angeles, CA, USA (P.L.)

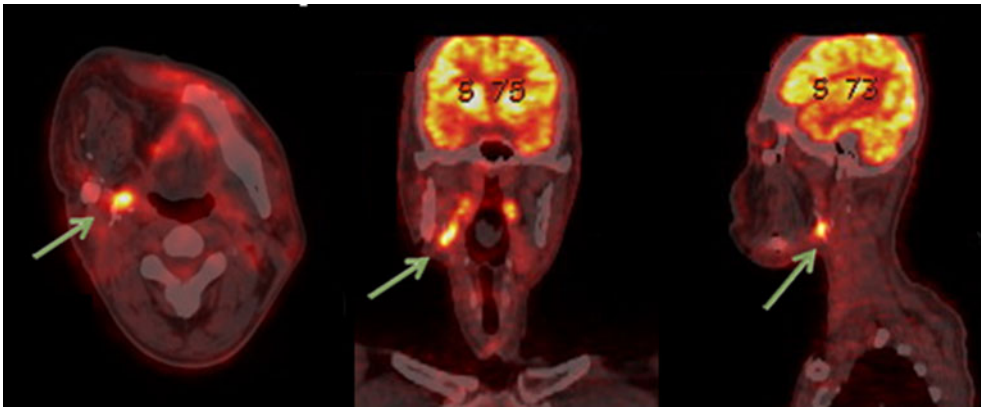

Fig. 2 Twelve-month follow-up PET/CT demonstrating a small FDG-avid recurrent lesion in the margin of the buccal flap from a previously treated T4N0 squamous buccal carcinoma. Image courtesy of Professor Tzu-chen Yen, Chang Gung Memorial Hospital, Linkou, Taiwan

discovered with neck dissection [10]. Thus, it remains unclear whether PET data can supplant CT evidence of lymphadenopathy when assessing residual disease.

The utility of PET/CT in assessing response to RT remains under investigation as well. Because of the high incidence of false positives (secondary to inflammation), PET screening generally begins 8–12 weeks after therapy. In a prospective study of 99 patients who received PET/CT 8 weeks after completing RT with or without chemotherapy for HNSCC, Moeller et al. found that combination PET/CT imaging was no better than CT imaging alone in predicting residual neck disease [11]. However, in a subgroup of patients with high risk of recurrence (i.e., those with HPV-negative tumors, nonpharyngeal primaries, and histories of alcohol and tobacco abuse), PET/CT had a positive predictive value of 75 and a NPV of 95 %. Based on those results, a positive PET/CT result following radiotherapy in patients at high risk of treatment failure likely necessitates a neck dissection, while a negative result is of debatable importance.

Kao et al. reported that negative PET/CT scans within 6 months served as a useful early predictor of response to radiotherapy [9]. Among 80 patients with stage II–IV HNSCC followed for an average of 21.8 months, the 2-year progression-free survival and overall survival (OS) rates were significantly different between patients who had a negative and those who had a positive PET/CT result within 6 months of the completion of RT (93 vs. 30 % [$p<0.001$] and 100 % vs. 32 % [$p<0.001$], respectively). Once again, PET scans had a poor positive predictive value, likely secondary to inflammation.

RT target volume delineation

PET- and CT-derived GTVs

Data suggest that GTV_{PET} are smaller but more accurate than traditional GTVs derived from CTs alone (GTV_{CT}) (Fig. 3). Improvement in delineating GTVs with integrated PET/CT was first demonstrated in 30 patients with HNSCC, for whom PET/CT had 97 % accuracy in delineating GTVs, compared with 69 % for CT and 40 % for MRI alone (the reference being a PET/MRI GTV) [12]. Ciernik et al. reported the first rigorous analysis of the effect of integrating PET/CT on contoured volumes [13]. GTV_{CT} differed significantly from GTV_{PET} in 56 % of 39 patients (12 with HNSCC). In 46 %, the planning target volume (PTV) changed by at least 20 %. Among HNSCC patients, GTV_{PET} were ≥25 % larger in 17 and ≥25 % smaller in 33 % of the patients. The use of PET/CT also significantly reduced interobserver variability.

Subsequent studies have generally found that GTV_{PET} are smaller than GTV_{CT} [4, 14–20]. One report compared

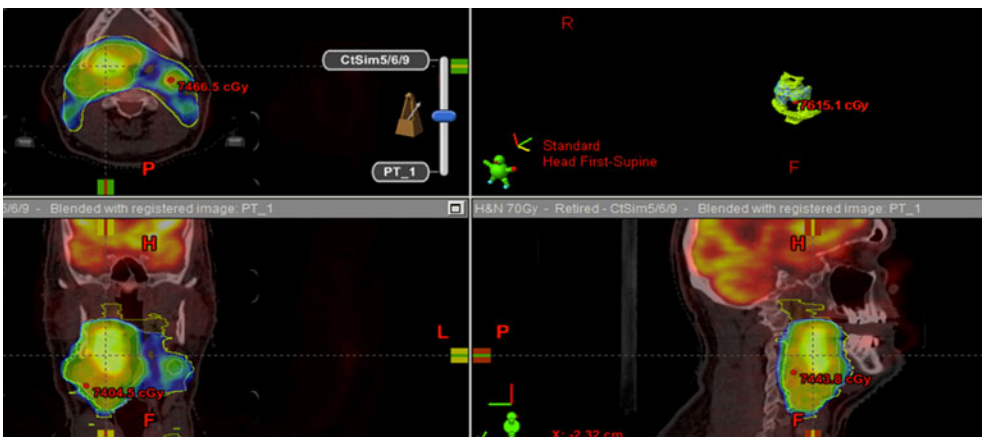

Fig. 3 GTV_{PET} in a patient with right base of tongue squamous cell carcinoma. Image courtesy of UCLA Department of Radiation Oncology, Los Angeles, CA, USA (P.L.)

GTV_{PET} in nine laryngeal carcinomas with GTVs derived from MRI and CT, as well as the pathologic tumor volume [19]. The investigators utilized a source-to-background (SBR) segmentation algorithm to delineate GTV_{PET} (discussed below) [21]. On average, imaging overestimated the true volume by 29, 65, and 89 % for PET, CT, and MRI, respectively. Most of the over-estimation involved the extra laryngeal and pre-epiglottic spaces and the thyroid. In spite of this, all three modalities also failed to include superficial mucosal extension of the tumor, amounting to nearly 10 % of the tumor volume. GTV_{CT} were 3.1 times larger than GTV_{PET} defined by windowing alone, though the integration of PET expanded nodal GTVs by 30 % [14].

GTV_{PET} were similarly found to be smaller than GTV_{CT} when delineated with a border criterion of 50 % of the maximum standardized uptake value (SUV; SUV_{50}; Fig. 4) [15]. However, in this study, the GTVs did not always overlap, and in 25 % of cases, the minimal dose received by 95 % of the GTV_{PET} was suboptimal. Similarly, in a study employing automatic segmentation for GTV_{PET}, the GTV_{PET} were 40 % smaller than GTV_{CT}, but mismatches were significant, with 45 % of patients having ≤15 % of the GTV_{PET} outside the GTV_{CT} [20]. Another group found similar results when comparing overall GTV_{PET} to GTV_{CT}, but not when comparing either nodal or primary GTVs [16]. In this report, PTV sizes were not changed from inclusion of PET data; however, the PTV configurations were altered. Finally, a recent study of 24 HNSCC patients found that visually contoured primary tumor GTV_{PET} were smaller than GTV_{CT} 80 % of the time, while out of 55 lymph node GTVs, there was no volumetric difference between modalities [4].

Albeit fewer in number, some studies have found that GTV_{PET} to be of similar volume compared with GTV_{CT} [13, 22, 23]. Additionally, a group who used a threshold of 40 % maximum SUV (SUV_{40}) for segmentation found that GTV_{PET} were significantly larger than GTV_{CT}, perhaps due to lack of FDG-uptake by peritumoral necrotic regions, or a SUV threshold effect [2]. In general, GTV_{PET} can be significantly mismatched with GTV_{CT}, which may be due to misregistration of the PET and CT images, and are often significantly smaller.

Segmentation strategies

The consistent discrepancies between GTV_{PET} and GTV_{CT} in these studies highlight the effect that incorporation of PET/CT into RT planning could have, and underscore the need for standardized segmentation strategies. Visual interpretation is commonly employed [14, 22, 24] but is highly sensitive to variations in windowing. Reigel et al. found significant differences between multiple observers contouring GTV_{PET} by visual interpretation [25]. Other strategies include a fixed SUV value (e.g., 2.5) [26], a fixed threshold level of the maximum SUV (SUV_{max}) value (e.g., SUV_{40}) [13, 15], or an adaptive threshold based off of the SBR [21]. In a series of 25 patients, the optimal SUV_{max} was found to be case based, with SUV_{20} and SUV_{40} appropriate for tumors with SUV >30 %±1.6 % kBq/mL and ≤30 %± 1.6 % kBq/mL, respectively [18]. In another report, no fixed threshold or SUV cutoff was deemed suitable in creating a GTV_{PET} that closely approximated GTV_{CT}, though a regression formula including tumor SUV_{max} was of benefit [27].

Schinagl et al. compared these various segmentation strategies in a cohort of 78 patients with HNSCC [28]. They found that contours based on these different strategies were highly variable, with using a fixed SUV value of 2.5 and above being a particularly poor method. On average, the threshold-based GTV_{PET} were smaller than GTV_{CT}, though rarely completely overlapping. Since the GTV_{CT} already included clinically detected peritumoral extension, some of the non-overlapping GTV_{PET} volume (accounting for up to 15–34 % of the GTV_{PET}) may include peritumoral inflammation.

Geets et al. subsequently proposed gradient-based segmentation that, in phantoms, proved more accurate than the

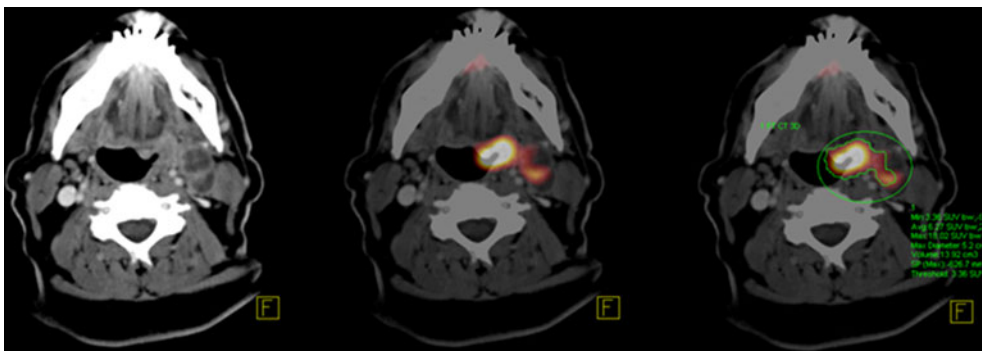

Fig. 4 Squamous cell carcinoma of the pharyngeal wall with adjacent lymph node metastases with necrotic center. PET/CT shows hypermetabolic primary carcinoma of pharyngeal wall with adjacent nodal metastases as well as example GTVs delineated with a threshold of SUV_{50}. Note that this threshold excludes much of the necrotic node. Image courtesy of M.D Anderson Cancer Center Orlando, Orlando, FL, USA

SBR method [21, 29]. In a pilot study of adaptive IMRT in ten patients, this gradient-based method was used to show that PET data allowed reduction in irradiated volumes of 15–40 % [17]. van Dalen et al. have also developed a background-subtracted relative-threshold level method, which obtained reliable thresholds independent of the signal-background-ratio in phantoms and two patients with liver metastases [30].

Few studies have evaluated segmentation strategies by comparing GTV_{PET} directly to pathologic tumor volumes. Importantly, most used frozen specimens and employed volumetric (e.g., ellipsoid) assumptions when calculating pathologic volumes, and thus these may not be appropriate gold standards. Nonetheless, these studies provide valuable information about the reliability and accuracy of various segmentation techniques. As discussed, Daisne et al. found that SBR-derived GTV_{PET} overestimated true pathologic volumes by 29 % in nine patients, though up to 10 % of the pathologic volume was missed [19]. Among 101 patients with oral cavity cancer a fixed SUV threshold of 3.5 was found to afford the best correlation between PET-derived GTV and pathologic volume (r^2=0.4) [31]. This was most pronounced for tumors extending ≥2 cm. Another group compared GTV_{PET} with pathologic volumes from 12 patients, and found that segmenting on SUV_{40} or on SUV= 2.5 grossly overestimated tumor volume, while narrowing the window by one SD of SUV_{max} or using a default value of ten underestimated the true volume [32]. The authors concluded that segmenting on SUV_{40}-generated volumes that correlated the best with pathologic volumes (r^2= 0.697), but this approximation was within ±50 % in only a third of the patients they studied, suggesting it is still a poor segmentation method.

Recently, Murphy et al. explored the relationship between various SUV-threshold derived GTV_{PET} and pathologic volumes in 23 patients with squamous cancer of the oral tongue [33]. The correlation between volumes was very poor for a wide range of thresholds (r^2=0.29–0.59). However, the SUV threshold that generated a GTV_{PET} equal to the pathologic volume was independently associated with both SUV_{max} and tumor grade. Because grade may vary within a tumor and has high inter- and intraobserver variability, its practical utility as a predictor is questionable. Table 1 summarizes current PET-based segmentation strategies with their known caveats. Overall, these results highlight the fact that current segmentation techniques poorly approximate the true tumor volume. Possibly, an integration of both a threshold SUV and a signal-to-background ratio based strategy might yield improved results.

Clinical results with PET/CT-guided therapy

Rothschild et al. published the first outcomes study of PET-guided RT for HNSCC patients, a matched case–control study with 45 patients treated with PET/CT-based IMRT and 86 patients treated with conformal RT [34]. The overall survival (OS) of patients with PET/CT-guided IMRT was 97 and 91 % at 1 and 2 years, respectively, compared to 74 and 54 % for patients without PET or IMRT (p=0.002). The event-free survival rate of PET/CT-IMRT group was 90 and 80 % at 1 and 2 years respectively, compared to 72 and 56 % in the control group (p=0.005). The use of IMRT rather than conformal RT could explain the different outcomes on its own, and the relative contribution of PET/CT-guidance is unclear. However, IMRT alone compared to conformal techniques often improves radiation toxicity endpoints rather than local control or survival, suggesting that PET may have a stronger impact on efficacy endpoints then the delivery technique. Another study reported OS and disease-free survival rates of 82.8 and 71.0 %, respectively, at 2 years, and 74.1 and 66.9 % at 3 years, among 42 patients treated with

Table 1 Segmentation strategies for PET-derived GTVs in HNSCC

Method	Notes	References
Visual interpretation	Significant interpersonal variations in target volume delineation among physicians.	[14, 22, 24, 25]
Fixed threshold SUV (e.g., SUV=2.5)	Most reports indicate that this method is fairly ineffective; although at least one study found segmenting on SUV=3.5 offered the best correlation between PET-derived GTVs and pathologic volumes.	[26, 28, 32]
% of SUV_{max} (e.g., SUV_{40})	The optimum % SUV cut-offs may be related to several factors: i.e. the absolute value of SUV_{max} or tumor grade. The regression term involving SUV_{max} may be helpful in tumor segmentation. However, this approach has also been found to overestimate tumor volumes.	[13, 15, 18, 27, 33]
SBR	The original SBR method overestimated true pathologic volume overall, but consistently underestimated mucosal extension. A more recent variation has been piloted in liver metastases.	[19, 30]
Gradient-based	Based off a computational model originally described in spherical phantom studies; this is the most recent method and is becoming more widely utilized.	[21, 29, 33]

SUV standardized uptake value, *SBR* signal-to-background ratio

PET/CT-guided RT [35]. Thirty-five of these patients received IMRT. Seven recurrences occurred after a mean duration of 9 months; SUV_{max} of either the GTV or nodal disease was not associated with recurrences. Therapy was well tolerated, and only 6 % of patients had acute grade 3 xerostomia.

PET signal changes during therapy

Measurable anatomic changes over a 5- to 7-week treatment course have been described in HNSCC patients, particularly after the third to fourth weeks [36]. Adaptive radiotherapy approaches could account for these volumetric changes. In a proof-of-concept study, Geets et al. found that around the foruth week of standard fractionation (i.e., after a dose of 30–40 Gy), the reliability of PET data declined, as the number of viable tumor cells dropped precipitously while peritumoral inflammation increased [17]. Another study tracked GTV_{PET} (segmented at SUV_{50}) in 23 patients and found that while median SUV decreased over time, the GTV_{PET} increased over time such that, beyond the delivery of 20 Gy, GTV_{PET} delineation was unreliable [37]. This increase is likely due to glucose-avid macrophages involved in radiation-induced inflammation. After extending the latter study to 37 patients, the rate of change in SUV_{max} from the time of 0 to 10/20 Gy was shown to be a prognostic factor for locoregional control and OS at 2 years, and the unreliability of GTV_{PET} beyond 20 Gy was confirmed [38].

Dose escalation

Patterns of local failure

As discussed, a paramount principle in RT for HNSCC involves delivering high dose to tumor while sparing dose to normal tissues. If the GTV_{PET} is a better indication of "true" tumor volume, then dose can be further escalated to this region, allowing for improved tumor control and better sparing of normal tissue (Fig. 5), such as the tissue flap in this previously irradiated patient. Before discussing the results of preliminary dose escalation studies, we briefly review the patterns of local failure. In a series of 61 patients treated with definitive 3D-CRT or IMRT, nine of nine local failures were located in-field, while one was located outside the GTV_{PET} [39]. While the PET imaging in this study was not obtained with patients in the same registration as during treatment, all images underwent deformable registration before analysis. Another group sequentially scanned 15 HNSCC patients before, during, and after radiotherapy to a median follow-up of 30.7 months [40]. All seven recurrences were in the GTV_{PET} (segmented by the SBR method). The group also employed hypoxic imaging with ^{18}F-fluoromisonidazole, and found that 57 % of recurrences occurred in hypoxic regions; the size and signal intensity of ^{18}F-fluoromisonidazole correlated negatively with survival.

In a retrospective review of 96 HNSCC patients, Wang et al. found that indeed, the majority (61.4 %) of stereotactic body radiotherapy (SBRT) failures were "near-misses" (20–75 % inside PTV or <20 % inside PTV, but closest edge within 1 cm of PTV) [41]. There was a significant improvement in OS and overlap/marginal failure-free survival among all patients with PET/CT-guided planning (log rank $p=0.037$) compared to patients with non PET/CT-guided planning. This was particularly true among patients receiving definitive RT ($n=89$; log rank $p=0.008$ and 0.009, respectively, for OS and overlap/marginal failure-free survival).

Preliminary results

Schwartz et al. investigated the approach of PET-based dose escalation in HNSCC by not covering neck levels that were PET negative [42]. In 20 HNSCC patients, the investigators created theoretical IMRT plans in which they limited the 66-Gy dose to FDG-positive clinical and nodal areas and in a subset of five of these patients, they boosted FDG-avid disease

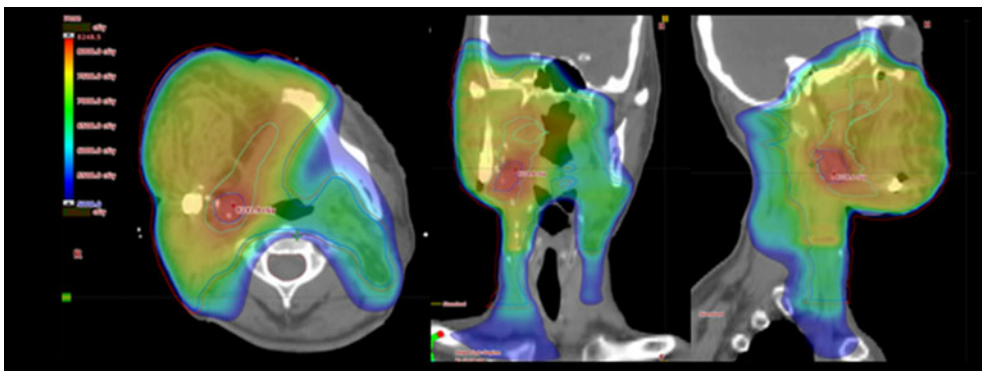

Fig. 5 A PET/CT-guided IMRT plan for the patient in Fig. 2 with a local recurrence of a T4N0 squamous buccal carcinoma. The overall plan was to deliver 72 Gy in 2-Gy fractions. A simultaneous integrated boost technique was used to boost the GTVPET (segmented by SUV_{50}) to 77.2 Gy. Image courtesy of Professor Tzu-chen Yen, Chang Gung Memorial Hospital, Linkou, Taiwan

with 0.5-cm margins in 2.2-Gy increments until dose-limiting criteria were reached. GTV_{PET} were segmented visually. Restriction of dose to PET-positive regions significantly reduced mean dose to the contralateral parotid and laryngeal cartilage in these theoretical plans, without missing pathologically verified nodal disease. Dose escalation allowed an increase in the dose covering 95 % of the PTV to a mean of 74.9 Gy; notably, patients with laryngeal cartilage or mandibular involvement were excluded due to limitation on dose escalation in these normal tissues. A subsequent phase I clinical trial investigated the uniform delivery of either 72 or 77 Gy to a PET-derived PTV (segmented by the SBR method) in 41 patients [43]. The trial was stopped early due to a non-radiation related death, but the authors concluded that a boost of 3 Gy/fraction to $\leq 10\ cm^3$ of the PET-avid region could be safely integrated in the first 2 weeks. Grade 3 dysphagia in 56 and 57 % of the 72- and 77-Gy groups respectively, was the major side effect. Complete response was observed in 86 and 81 % of the 72- and 77-Gy groups, respectively, with 1-year OS of 82 and 54 %. In four of the nine patients with recurrences, the disease relapsed in the boosted PET-avid region.

Another group utilized a voxel intensity-based/dose painting by the numbers (DPBN) approach to dose escalation, wherein the dose to a region including the GTV_{PET} (segmented by the SBR method) varied in proportion to the intensity of the PET signal [44]. Notably, they set the low end of the intensity threshold at 25 % of the high-end threshold (the 95th percentile of intensity values); thus dose escalation was focused to smaller volumes for more pronounced intensity peaks. Compared with a simple contour-based approach, the DPBN approach developed sharper peak-dose regions with the target volume in 15 HNSCC patients. The same group subsequently combined adaptive IMRT with DPBN in 21 HNSCC patients [45]. Each patient received three separate plans: fractions 1–10 used a pretreatment PET scan for DPBN, fractions 11–20 used a PET scan after the eighth fraction for DPBN, and fractions 21–32 used a uniform IMRT plan. In seven patients, the PET-derived clinical target volume (CTV_{PET}) (segmented at SUV_{50}) received 80.9 Gy; in 14 others, the GTV_{PET} received 85.9 Gy. No patients had grade 4 toxicity or required treatment breaks. The adaptation of treatment by the second PET scan reduced the volumes of the GTV_{PET} (41 %), CTV_{PET} (18 %), high-dose PTV (14 %), and parotids (9–12 %). In fact, due the smaller target volume at 85.9 Gy, the patients receiving higher dose actually had less acute toxicity than those receiving 80.9 Gy. Thus, DPBN based on PET-derived volumes is promising and may be safe and effective.

Conclusion

PET/CT- based imaging for HNSCC provides several significant advantages for radiation oncologists. First, it modifies staging information in nearly 40 % of cases, thus modifying therapeutic goals. Second, it may assist in disease surveillance and the assessment of treatment response. Third, it allows for delineation of GTVs that appear to correlate more closely with "true" pathologic tumor volumes. These are generally significantly smaller than GTV_{CT}, but are not necessarily overlapping. Based on the premise that these GTV_{PET} represent "true", biologically active tumor, PET/CT allows for dose escalation that, in preliminary studies, is well tolerated. PET/CT can be further used in adaptive RT planning, albeit only in the first half of treatment. A key issue in the future of employing PET/CT for RT planning is the appropriate method for segmenting the PET signal to reliably delineate GTV_{PET}. Once a segmentation protocol is standardized, PET/CT planning appears to represent an exciting, biologically based tool in the radiation oncologists' armamentarium in treating HNSCC.

Conflict of interest None to disclose

References

1. Dietl B, Marienhagen J, Kuhnel T, Schreyer A, Kolbl O (2008) Oral Oncol 44(5):504
2. Deantonio L, Beldi D, Gambaro G, Loi G, Brambilla M, Inglese E, Krengli M (2008) Radiat Oncol (London, England) 3:29
3. Scott AM, Gunawardana DH, Bartholomeusz D, Ramshaw JE, Lin P (2008) J Nucl Med: Official Publication, Society of Nuclear Medicine 49(10):1593
4. Delouya G, Igidbashian L, Houle A, Belair M, Boucher L, Cohade C, Beaulieu S, Filion EJ, Coulombe G, Hinse M, Martel C, Despres P, Nguyen-Tan PF (2011) Radiother Oncol: Journal of the European Society for Therapeutic Radiology and Oncology 101(3):362
5. Lonneux M, Hamoir M, Reychler H, Maingon P, Duvillard C, Calais G, Bridji B, Digue L, Toubeau M, Gregoire V (2010) J Clin Oncol: Official Journal of the American Society of Clinical Oncology 28(7):1190
6. Kyzas PA, Evangelou E, Denaxa-Kyza D, Ioannidis JP (2008) J Natl Cancer Inst 100(10):712
7. Nayak JV, Walvekar RR, Andrade RS, Daamen N, Lai SY, Argiris A, Smith RP, Heron DE, Ferris RL, Johnson JT, Branstetter BFT (2007) Laryngoscope 117(12):2129
8. Ong SC, Schoder H, Lee NY, Patel SG, Carlson D, Fury M, Pfister DG, Shah JP, Larson SM, Kraus DH (2008) J Nucl Med: Official Publication, Society of Nuclear Medicine 49(4):532
9. Kao J, Vu HL, Genden EM, Mocherla B, Park EE, Packer S, Som PM, Kostakoglu L (2009) Cancer 115(19):4586
10. Waldron JN, Gilbert RW, Eapen L, Hammond A, Hodson DI, Hendler A, Perez-Ordonez B, Gu C, Julian JA, Julian DH, Levine MN (2011) J Clin Oncol: Official Journal of the American Society of Clinical Oncology 29(suppl: abstr 5504)
11. Moeller BJ, Rana V, Cannon BA, Williams MD, Sturgis EM, Ginsberg LE, Macapinlac HA, Lee JJ, Ang KK, Chao KS, Chronowski GM, Frank SJ, Morrison WH, Rosenthal DI, Weber RS, Garden AS, Lippman SM, Schwartz DL (2009) Journal of Clin Oncol: Official Journal of the American Society of Clinical Oncology 27(15):2509

12. Wong WL, Hussain K, Chevretton E, Hawkes DJ, Baddeley H, Maisey M, McGurk M (1996) Am J Surg 172(6):628
13. Ciernik IF, Dizendorf E, Baumert BG, Reiner B, Burger C, Davis JB, Lutolf UM, Steinert HC, Von Schulthess GK (2003) Int J Radiat Oncol Biol Phys 57(3):853
14. Heron DE, Andrade RS, Flickinger J, Johnson J, Agarwala SS, Wu A, Kalnicki S, Avril N (2004) Int J Radiat Oncol Biol Phys 60(5):1419
15. Paulino AC, Koshy M, Howell R, Schuster D, Davis LW (2005) Int J Radiat Oncol Biol Phys 61(5):1385
16. Guido A, Fuccio L, Rombi B, Castellucci P, Cecconi A, Bunkheila F, Fuccio C, Spezi E, Angelini AL, Barbieri E (2009) Int J Radiat Oncol Biol Phys 73(3):759
17. Geets X, Tomsej M, Lee JA, Duprez T, Coche E, Cosnard G, Lonneux M, Gregoire V (2007) Radiother Oncology: Journal of the European Society for Therapeutic Radiology and Oncology 85(1):105
18. El-Bassiouni M, Ciernik IF, Davis JB, El-Attar I, Reiner B, Burger C, Goerres GW, Studer GM (2007) Int J Radiat Oncol Biol Phys 69(1):286
19. Daisne JF, Duprez T, Weynand B, Lonneux M, Hamoir M, Reychler H, Gregoire V (2004) Radiology 233(1):93
20. Henriques de Figueiredo B, Barret O, Demeaux H, Lagarde P, De-Mones-Del-Pujol E, Kantor G, de Clermont-Gallerande H, Richaud P, Fernandez P (2009) Radiother Oncol: Journal of the European Society for Therapeutic Radiology and Oncology 93(3):479
21. Daisne JF, Sibomana M, Bol A, Doumont T, Lonneux M, Gregoire V (2003) Radiother Oncol: Journal of the European Society for Therapeutic Radiology and Oncology 69(3):247
22. Nishioka T, Shiga T, Shirato H, Tsukamoto E, Tsuchiya K, Kato T, Ohmori K, Yamazaki A, Aoyama H, Hashimoto S, Chang TC, Miyasaka K (2002) Int J Radiat Oncol Biol Phys 53(4):1051
23. Ahn PH, Garg MK (2008) Semin Nucl Med 38(2):141
24. Nestle U, Schaefer-Schuler A, Kremp S, Groeschel A, Hellwig D, Rube C, Kirsch CM (2007) Eur J Nucl Med Mol Imaging 34 (4):453
25. Riegel AC, Berson AM, Destian S, Ng T, Tena LB, Mitnick RJ, Wong PS (2006) Int J Radiat Oncol Biol Phys 65(3):726
26. Hong R, Halama J, Bova D, Sethi A, Emami B (2007) Int J Radiat Oncol Biol Phys 67(3):720
27. Kao CH, Hsieh TC, Yu CY, Yen KY, Yang SN, Wang YC, Liang JA, Chien CR, Chen SW (2010) Radiat Oncol (London, England) 5:76
28. Schinagl DA, Vogel WV, Hoffmann AL, van Dalen JA, Oyen WJ, Kaanders JH (2007) Int J Radiat Oncol Biol Phys 69(4):1282
29. Geets X, Lee JA, Bol A, Lonneux M, Gregoire V (2007) Eur J Nucl Med Mol Imaging 34(9):1427
30. van Dalen JA, Hoffmann AL, Dicken V, Vogel WV, Wiering B, Ruers TJ, Karssemeijer N, Oyen WJ (2007) Nucl Med Commun 28(6):485
31. Baek CH, Chung MK, Son YI, Choi JY, Kim HJ, Yim YJ, Ko YH, Choi J, Cho JK, Jeong HS (2008) J Nucl Med: Official Publication, Society of Nuclear Medicine 49(9):1422
32. Burri RJ, Rangaswamy B, Kostakoglu L, Hoch B, Genden EM, Som PM, Kao J (2008) Int J Radiat Oncol Biol Phys 71 (3):682
33. Murphy JD, Chisholm KM, Daly ME, Wiegner EA, Truong D, Iagaru A, Maxim PG, Loo BW Jr, Graves EE, Kaplan MJ, Kong C, Le QT (2011) Radiother Oncol: Journal of the European Society for Therapeutic Radiology and Oncology 101(3):356
34. Rothschild S, Studer G, Seifert B, Huguenin P, Glanzmann C, Davis JB, Lutolf UM, Hany TF, Ciernik IF (2007) Radiat Oncol (London, England) 2:22
35. Vernon MR, Maheshwari M, Schultz CJ, Michel MA, Wong SJ, Campbell BH, Massey BL, Wilson JF, Wang D (2008) Int J Radiat Oncol Biol Phys 70(3):678
36. Barker JL Jr, Garden AS, Ang KK, O'Daniel JC, Wang H, Court LE, Morrison WH, Rosenthal DI, Chao KS, Tucker SL, Mohan R, Dong L (2004) Int J Radiat Oncol Biol Phys 59(4):960
37. Hentschel M, Appold S, Schreiber A, Abramyuk A, Abolmaali N, Kotzerke J, Baumann M, Zophel K (2009) Int J Radiat Biol 85 (9):796
38. Hentschel M, Appold S, Schreiber A, Abolmaali N, Abramyuk A, Dorr W, Kotzerke J, Baumann M, Zophel K (2011) Eur J Nucl Med Mol Imaging 38(7):1203
39. Soto DE, Kessler ML, Piert M, Eisbruch A (2008) Radiother Oncol: Journal of the European Society for Therapeutic Radiology and Oncology 89(1):13
40. Dirix P, Vandecaveye V, De Keyzer F, Stroobants S, Hermans R, Nuyts S (2009) J Nucl Med: Official Publication, Society of Nuclear Medicine 50(7):1020
41. Wang K, Heron DE, Flickinger JC, Rwigema JC, Ferris RL, Kubicek GJ, Ohr JP, Quinn AE, Ozhasoglu C, Branstetter BF (2012) Head Neck Oncol 4(1):12
42. Schwartz DL, Ford EC, Rajendran J, Yueh B, Coltrera MD, Virgin J, Anzai Y, Haynor D, Lewellen B, Mattes D, Kinahan P, Meyer J, Phillips M, Leblanc M, Krohn K, Eary J, Laramore GE (2005) Head Neck 27(6):478
43. Madani I, Duthoy W, Derie C, De Gersem W, Boterberg T, Saerens M, Jacobs F, Gregoire V, Lonneux M, Vakaet L, Vanderstraeten B, Bauters W, Bonte K, Thierens H, De Neve W (2007) Int J Radiat Oncol Biol Phys 68(1):126
44. Vanderstraeten B, Duthoy W, De Gersem W, De Neve W, Thierens H (2006) Radiother Oncol: Journal of the European Society for Therapeutic Radiology and Oncology 79(3):249
45. Duprez F, De Neve W, De Gersem W, Coghe M, Madani I (2011) Int J Radiat Oncol Biol Phys 80(4):1045